Time-Dependent Morphology Development in a Segmented Polyurethane with Monodisperse Hard Segments Based on 1,4-Phenylene Diisocyanate

Jignesh P. Sheth,[†,§] Derek B. Klinedinst,[†] Todd W. Pechar,[†] Garth L. Wilkes,[*,†] Emel Yilgor,[‡] and Iskender Yilgor[‡]

Department of Chemical Engineering, Virginia Polytechnic Institute & State University, Blacksburg, Virginia 24061, and Department of Chemistry, Koc University, Istanbul 34450, Turkey

Received May 24, 2005; Revised Manuscript Received September 12, 2005

ABSTRACT: The time-dependent morphology development in a segmented polyurethane, which was prepared by the reaction of equimolar amounts of 1,4-phenylene diisocyanate (*p*PDI) and poly(tetramethylene oxide)glycol of $\langle M_n \rangle$ of 975 g/mol, was investigated. No chain extender was utilized during the synthesis, and the resultant monodisperse hard segments constituted 14 wt % of the copolymer. Time-dependent microphase separation and morphology development was studied at room temperature by using solvent-cast films which were heated above the hard segment melting temperature, 55 °C, to erase the semicrystalline microphase morphology. Atomic force microscopy showed that, following heat treatment, the hard phase first developed into short rods within 30 min, followed by a growth period during which the short rods grew longer and eventually into a well-defined percolated structure. Morphology development was also followed by FTIR spectroscopy. While the intensity of the free C=O peak at 1730 cm^{-1} decreased, the intensity of the hydrogen-bonded C=O peak at 1695 cm^{-1}, which was not present in the original annealed sample, increased with time and began to plateau in ~24 h. A time-dependent increase in the storage modulus of the copolymer, following heat treatment, was also noted. This latter change could be described by the Avrami equation, yielding an Avrami exponent of 0.55. Because of the similarity of the copolymer's morphology to that of short fiber reinforced polymer composites, selected models developed for predicting the modulus of such composites could reasonably estimate the initially surprisingly high ambient temperature storage modulus of the copolymer of 0.9×10^8 Pa.

Introduction

Segmented, thermoplastic polyurethanes are generally synthesized via a one- or two-step approach. Polyurethanes intended for structural applications usually require a relatively high hard segment content, which is achieved in the above reaction strategies by utilizing a chain extender.[1,2] We recently synthesized segmented polyurethanes and polyureas possessing ~14 wt % hard segment content in a single step without using a chain extender.[3] These particular materials were produced in solution by reacting equimolar amounts of a selected diisocyanate with a hydroxyl-terminated or an amine-terminated poly(tetramethylene oxide) (PTMO) of ca. $\langle M_n \rangle$ 1000 g/mol. Investigation of the solid-state structure−property behavior of these materials indicated that a proper selection of the level of symmetry and/or cohesiveness of the hard microdomains may allow elimination of the traditional requirement of chain extension to obtain melt-processable segmented urethanes and, more specifically, urea copolymers with useful structural properties.[3−5] In those studies various diisocyanates, such as 1,4-phenylene diisocyanate (*p*PDI), 1,3-phenylene diisocyanate, 2,4-toluene diisocyanate, 2,6-toluene diisocyanate, diphenylmethane diisocyanate, hydrogenated diphenylmethane diisocyanate, *trans*-1,4-cyclohexane diisocyanate, and 1,6-hexamethylene diisocyanate, were used. The reaction scheme to produce the *p*PDI based segmented polyurethane with PTMO as the soft segment (PTMO-*p*PDI-U) is presented in Scheme 1. A detailed description of the synthesis procedure is given elsewhere.[3] Copolymers produced according to Scheme 1 possess hard segments based on only a single diisocyanate molecule; that is, *no chain extenders are utilized*.

In the present report, the time-dependent development of a microphase-separated morphology from a disordered state in the copolymer PTMO-*p*PDI-U is discussed. Tapping-mode atomic force microscopy (AFM) is used to visually follow the time-dependent morphology development. The concurrent formation of the hydrogen-bonded network and the corresponding increase in the stiffness of this sample, each separately monitored by utilizing FTIR spectroscopy in attenuated total reflectance mode (ATR−FTIR) and dynamic mechanical analysis (DMA), respectively, are also presented. The sample PTMO-*p*PDI-U was selected because it softens (see below) over a temperature range that enables the use of AFM, FTIR, and DMA to conveniently monitor the morphology development in the sample at ambient temperature.

Experimental Section

Sample Preparation. As noted earlier, the synthesis of PTMO-*p*PDI-U (Scheme 1) is given elsewhere.[3] A solution-cast film of this sample, ~1 mm thick, was prepared by pouring the copolymer solution (20 wt % solids in dimethylformamide) into a poly(tetrafluoroethylene) mold. The mold was covered with a glass Petri dish to slow down the solvent evaporation and then placed in an oven at 60 °C. After the bulk of the solvent had evaporated, the mold was placed in a vacuum oven maintained at 60 °C, for complete drying, which was monitored gravimetrically. The resulting film was stored under vacuum at room temperature until needed for testing.

[†] Virginia Polytechnic Institute & State University.
[‡] Koc University.
[§] Current address: Xerox Corporation, 26600 SW Parkway Ave., Wilsonville, OR 97070.
* To whom correspondence should be addressed: Tel 1-540-231-5498; Fax 1-540-231-9511; e-mail gwilkes@vt.edu.

10.1021/ma051063a CCC: $30.25
Published on Web 11/04/2005

Scheme 1

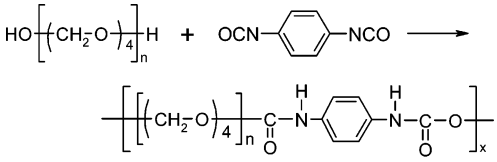

Segmented Polyurethane Copolymer, PTMO-*p*PDI-U

Differential Scanning Calorimetry (DSC). The heating scans of a solvent-cast film of PTMO-*p*PDI-U DSC were collected by using a Seiko DSC 220C. The heating rate was maintained at 10 °C/min throughout the experiment. For the first heating scan, the sample was heated to a temperature just above its melting transition, around 55 °C. Thereafter, it was cooled to room temperature at 10 °C/min, aged for 4 h, and reheated to 100 °C to collect the second heating scan. Consequently, third and fourth heating scans of this same sample, aged at room temperature for 12 and 96 h, respectively, were also collected. Note that between the second and the third heating scans the sample was allowed to cool to room temperature without any forced cooling.

Wide-Angle X-ray Scattering (WAXS). Two-dimensional WAXS patterns of PTMO-*p*PDI-U were collected by using a Philips PW 1720 X-ray diffractometer emitting Cu Kα radiation with a wavelength, λ of 1.54 Å. The operating voltage and the tube current were set at 40 kV and 20 mA, respectively. The sample-to-film distance was set at 47.3 mm, and the pattern was exposed on Kodak Biomax MS film in an evacuated sample chamber for 4 h. Sample thickness was on the order of 150 μm.

Dynamic Mechanical Analysis (DMA). A rectangular sample (10 × 3 mm^2) of PTMO-*p*PDI-U was cut from the thoroughly dried film and used for DMA measurement, conducted in a Seiko model DMS210 instrument. The sample was quenched from room temperature to −100 °C using liquid nitrogen and thereafter subjected to a heating scan at 2 °C/min under a dry nitrogen blanket. The E' and tan δ profiles were collected at a frequency of 1 Hz. The time-dependent E' values were measured at ambient temperature.

Tapping-Mode Atomic Force microscopy (AFM). Phase images were captured at ambient temperature by using a Digital Instruments (now Veeco) Dimension 3000 AFM equipped with a NanoScope IIIa controller. Nanodevices TAP150 probes with a spring constant 5 N/m and a resonant frequency in the vicinity of 100 kHz were used. The samples were imaged at a frequency of 1 Hz and a set point ratio of ∼0.6.

Fourier Transform Infrared Spectroscopy (FTIR). A BIO-RAD FTS-40A spectrophotometer was used to collect FTIR data in the attenuated total reflectance (ATR) mode. The instrument was equipped with a liquid nitrogen cooled MCT detector. All spectra were collected using 64 scans at 2 cm^{-1} resolution. A KRS-5 internal reflection element, from Harrick Scientific Corp., with dimensions of 50 × 10 × 3 mm^3 was used as the ATR crystal.

Results and Discussion

The temperature-dependent storage modulus, E', and tan δ responses of PTMO-*p*PDI-U (Figure 1) indicate that the copolymer possesses a microphase-separated morphology up to ∼50 °C. In particular, the E' response indicates a soft segment glass transition at about −70 °C, as expected for the PTMO soft segment. Note that microphase-separated copolymers based on PTMO typically display a soft segment T_g in the range of −70 °C when there is little hard−soft segmental mixing.[1,2] Following the soft segment glass transition the E' response displays a rubbery plateau with a value in the range of 10^8 Pa. The high average E' values above the soft segment T_g are more commonly exhibited by conventional chain extended polyurethanes with a distinctly higher hard segment content than the

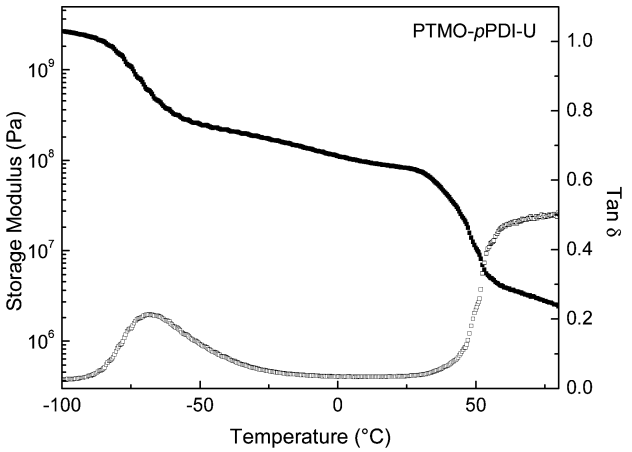

Figure 1. DMA behavior of solution-cast film from a 20 wt % solution in dimethylformamide.

14 wt % present in PTMO-*p*PDI-U.[2] Such behavior strongly alludes to the presence of long-range connectivity of the hard segments and the percolation of the hard phase through the soft matrix as was shown in our earlier report.[3] The observation of neck formation and a yield point in this sample, when it is uniaxially stretched at ambient temperature, indirectly supports the above statement. Note that, during the second tensile deformation cycle immediately following the first, PTMO-*p*PDI-U displayed high elongation at break and low mechanical hysteresis[4] which is often typical of elastomeric materials. The tan δ response of PTMO-*p*PDI-U (Figure 1) displays a damping peak centered at −70 °C which corresponds to the soft segment T_g. The increase in the tan δ response above 45 °C corresponds to a drop in E', a behavior that arises due to the softening of the sample and which is caused by the melting of the hard segment phase. The crystalline nature of the *p*PDI-based hard phase is evident from the WAXS and DSC results presented in Figure 2. The wide-angle X-ray scattering pattern (Figure 2a) of the as-cast and fully aged PTMO-*p*PDI-U shows a reasonably sharp, azimuthally independent reflection due to the crystalline hard segments. The DSC heating scan (Figure 2b) of this sample shows a melting endotherm centered around 50 °C, which corresponds to the transition observed in DMA (Figure 1). Note that *pure hydroxyl end-capped* PTMO of $\langle M_n \rangle$ 1000 g/mol completes it melting transition by ca. 25 °C (data not shown). Therefore, the above-noted melting endotherm is distinctly due to the crystalline hard segments and not the PTMO-based soft segment phase. The second heating scan of PTMO-*p*PDI-U (Figure 2b), which was aged for 4 h at room temperature, also shows a melting endotherm centered around 50 °C. The intensity and the area under this peak systematically grow with aging time (heating scans at 12 and 96 h are shown), thereby alluding to a time-dependent morphology development in this sample. Such time-dependent behavior is explored in further detail with AFM and DMA later in this report.

Direct support for the presence of hard segment long-range connectivity is provided by AFM (Figure 3, reproduced from ref 3). The phase image of PTMO-*p*PDI-U displays a distinctly percolated hard phase that has developed into curved rodlike hard domains of high aspect ratio. These curved rods, which are crystalline and randomly dispersed throughout the soft matrix, enable the rubbery plateau of the sample to exhibit a

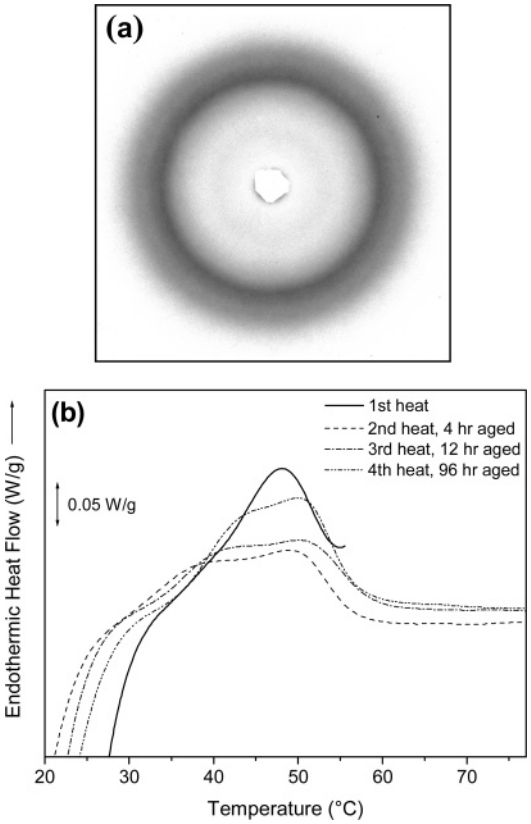

Figure 2. (a) WAXS pattern of solution-cast and fully aged PTMO-*p*PDI-U. (b) DSC heating scans of PTMO-*p*PDI-U that was aged for various lengths of time, as indicated in the legend.

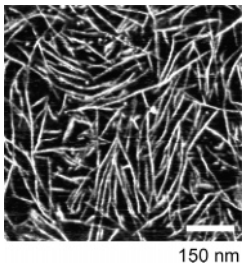

Figure 3. Ambient temperature tapping-mode AFM phase image of the free surface of PTMO-*p*PDI-U solution-cast film. Note that, in addition to the free surface, tapping-mode AFM tends to image a few nanometers underneath the surface. Thus, hard domains just below the free surface also contribute to the phase image, thereby producing a micrograph that appears to display a higher content of the hard phase than actually present, 14 wt %. Figure reproduced with permission from ref 3. Copyright 2005 Elsevier.

high average E'. Hence, these hard domains could be perceived to be similar to randomly dispersed fibers of high aspect ratio in a fiber-reinforced composite. If such an analogy is valid, then it should be possible to predict the tensile modulus of this segmented copolymer by utilizing models previously proposed for predicting the tensile modulus of a fiber-reinforced composite containing randomly oriented short fibers. There are many models available in the literature, and those proposed by Cox, Christensen, and Pan are considered.[7] Among these three models, the former two appear to be the most frequently utilized to model fiber-reinforced composites with short fibers randomly oriented in two (2D) or all three (3D) directions. The mathematical equations for the three models are presented in Table 1. The predicted composite modulus, the fiber modulus, and the matrix modulus are represented by the variables E_c, E_f, and E_m, respectively. The fiber volume fraction is represented by v_f.

The tensile modulus of a glassy polymer is generally in the range of $(1-8) \times 10^9$ Pa, and that of a rubbery polymer generally ranges between 1 and 10×10^5 Pa.[8] Hence, E_f and E_m values of 5×10^9 and 5×10^5 Pa can be reasonably assumed. It is evident from Table 1 that the three models are very sensitive to E_f and quite insensitive to E_m. In fact, the Cox model completely disregards the matrix modulus, E_m. The hard segment weight fraction can be approximately converted to volume fraction by using the densities of PTMO and *p*PDI. This conversion assumes that the density of the soft and the hard phases in the copolymer are equal to their respective precursors, an assumption that may not be completely valid. The density of PTMO of $\langle M_n \rangle$ 1000 g/mol is 0.97−0.98 g/cm^3, and that of *p*PDI is 1.16−1.17 g/cm^3. Thus, the 14 wt % hard segment content of the copolymer translates to a v_f of about 0.12. Note that the above conversion also assumes complete phase separation between the hard and the soft phases, which may not necessarily be the case (see below). The tensile modulus of the copolymer (or composite) with fibers oriented randomly in 2D or 3D is calculated by using the above three models to be approximately 2×10^8 and 1×10^8 Pa, respectively.

The sample PTMO-*p*PDI-U possesses an ambient temperature Young's modulus of 0.3×10^8 Pa.[4] In addition, its ambient temperature storage modulus (Figure 1) is 0.9×10^8 Pa. This close agreement between the measured modulus and that predicted by the three models is a little surprising, especially in light of the limiting assumptions noted above and an absence of the dispersed phase (fibers) aspect ratio as a parameter in the three models. Nonetheless, the above analysis confirms the earlier conclusion that in this segmented copolymer the hard, curved rodlike crystalline phase, just like fibers in polymer composites, reinforces the "soft" matrix. Similar analysis was found to be valid for *p*PDI- and 1,3-phenylene diisocyanate (*m*PDI)-based segmented polyureas, two copolymers not considered in this paper.

As discussed above, the hard segment crystalline phase in PTMO-*p*PDI-U melts at ~50 °C. Consequently, at ambient temperature the melt-processed sample experiences a supercooling of only about 25 °C. Thus, AFM is especially suitable to monitor the crystallization and morphological development in the sample at ambient temperature after cooling PTMO-*p*PDI-U from the melt. The solution-cast film of this copolymer was heated to 55 °C for 15 min to fully erase its hard phase order. The melted sample was then allowed to cool to ambient temperature and thereafter kept at this temperature during all subsequent measurements. Tapping-mode AFM was then utilized to image a selected region of the film's free surface at different time intervals (Figure 4). The first phase image (not shown), taken 15 min after the sample was removed from the oven, was uniformly dark and without the presence of any light regions or, in other words, hard domains. This image suggests that in PTMO-*p*PDI-U there is very little microphase separation, if any, within the first 15 min after heat treatment. The next image, taken after 30 min, exhibited bright and dark regions, which are indicative of a microphase-separated morphology. These bright regions or hard domains were rodlike in shape,

Table 1. Mathematical Models To Predict the Modulus of Fiber-Reinforced Composites

model	2D random	3D random
Cox	$E_c^{2D} = (v_f/3)E_f$	$E_c^{3D} = (v_f/6)E_f$
	($E_c^{2D} = 200 \times 10^6$ Pa)[a]	($E_c^{3D} = 100 \times 10^6$ Pa)
Christensen	$E_c^{2D} = (v_f/3)E_f + (1 + v_f)E_m$	$E_c^{3D} = (v_f/6)E_f + [1 + (1 + v_f)]E_m$
	($E_c^{2D} = 201 \times 10^6$ Pa)	($E_c^{3D} = 101 \times 10^6$ Pa)
Pan	$E_c^{2D} = (v_f/\pi)E_f + (1 - v_f/\pi)E_m$	$E_c^{3D} = (v_f/2\pi)E_f + (1 - v_f/2\pi)E_m$
	($E_c^{2D} = 191 \times 10^6$ Pa)	($E_c^{3D} = 96 \times 10^6$ Pa)

[a] Calculated modulus values of PTMO-*p*PDI-U are provided in brackets.

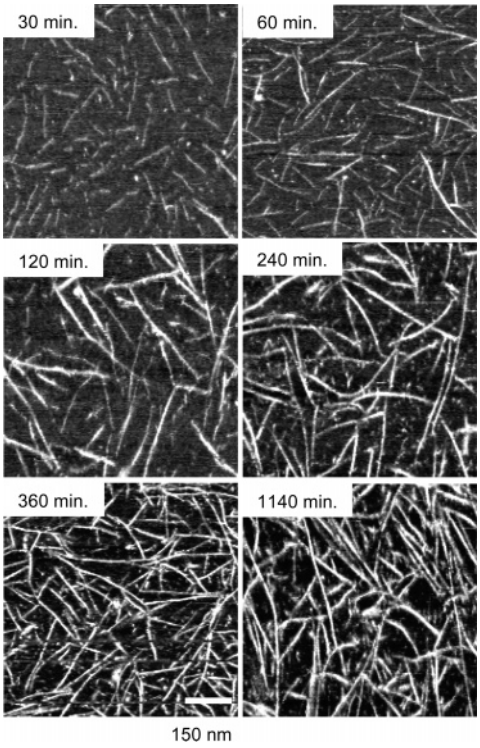

Figure 4. Ambient temperature tapping-mode AFM phase images of PTMO-*p*PDI-U captured at various times following heat treatment. Above phase images were captured from within a region 7 μm $\times$ 7 μm. Approximately 8 min was required to capture each AFM image.

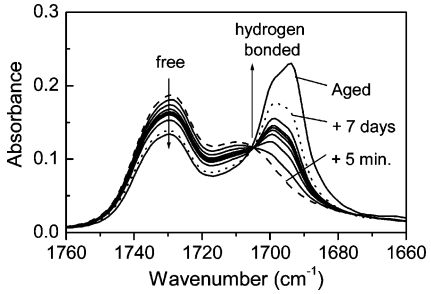

Figure 5. Infrared absorbance of PTMO-*p*PDI-U within the urethane C=O stretching region, at various times following heat treatment. The spectra were corrected for baseline differences and normalized by using the ⟩C=C⟨ absorbance at 1600 cm^{-1}.

and they progressively increased in length with time. It is not clear from the data presented thus far whether microphase separation precedes hard segment crystallization or whether hard segment crystallization induces microphase separation. The authors are currently gathering synchrotron X-ray data to ascertain this fact. Note that as discussed, above the hard domains are crystalline. After 6 h the resultant curved rodlike hard domains appear throughout the soft matrix. The sample's morphology after further elapse of time (1140 min or 19 h) did not differ greatly from that after 6 h. Such behavior indicates that at ambient temperature most of the morphological development on the surface of PTMO-*p*PDI-U, as resolved by the AFM technique, is accomplished in about 6 h, at these conditions. More importantly, aside from slight differences in the packing density of the curved rodlike hard domains, the morphology in the sample after 19 h is beginning to closely resemble that of the original solution-cast sample (Figure 3) that was allowed to age for 1 week at ambient temperature.

The development of the hydrogen-bonded network within the hard phase of PTMO-*p*PDI-U following heat treatment was also monitored by using ATR−FTIR spectroscopy. A sample of PTMO-*p*PDI-U was cut from the larger copolymer film to identical dimensions as the ATR crystal and placed onto the crystal, and both were heated at 60 °C for 30 min in an oven. The assembly was then removed and immediately placed into the ATR cell for data collection. The time-dependent change in the absorbance intensity within the carbonyl region of PTMO-*p*PDI-U is presented in Figure 5. As clearly seen in this figure, at $t = 5$ min, that spectrum shows a strong absorption at 1730 cm^{-1} (free C=O) and a slight shoulder at 1710 cm^{-1} (loosely H-bonded C=O). Interestingly, in this sample the strongly hydrogen-bonded and ordered C=O peak, at 1700 cm^{-1}, is absent. As the sample is aged at ambient temperature the 1730 cm^{-1} peak slowly becomes smaller, and a well-defined peak at 1700 cm^{-1} starts appearing after about 120 min. This indicates the formation of an ordered hard segment phase. A steady increase in the 1700 cm^{-1} peak and a continued decrease in absorbance values of 1730 cm^{-1} peak are observed thereafter. The FTIR study indicates that the hydrogen-bonded network formation begins to reach a plateau in about 24 h (see below), under ambient conditions. However, even after 7 days there is a substantial amount of non-hydrogen-bonded hard segments as indicated by the absorbance value at 1700 cm^{-1}. This indicates a limited mixing between hard and the soft segments in addition to the presence of well-separated hard segment phase and soft segment phase. The broad MWD of the PTMO-975 precursor, ~2, results in some soft segments in PTMO-*p*PDI-U that are substantially shorter than the average. These short soft segments may be expected to contribute to some limited phase mixing between the soft and the hard phase.

The development of the ambient temperature time-dependent morphology throughout the bulk of the copolymer was also confirmed by monitoring the storage modulus of PTMO-*p*PDI-U (Figure 6). The sample utilized for DMA was subjected to a thermal treatment identical to that in the above two techniques. The copolymer was slightly tacky upon reaching ambient temperature. However, after 15 min, the value of E' of the sample was measured to be 0.9×10^7 Pa. It rose

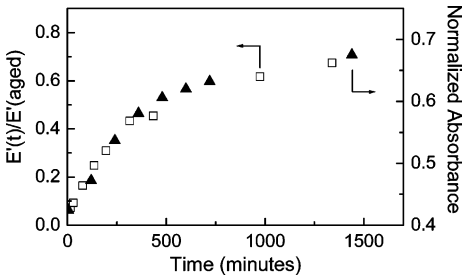

Figure 6. Change in the normalized storage modulus and the normalized peak absorbance of the hydrogen-bonded urethane C═O of PTMO-*p*PDI-U over a period of ~24 h. The peak absorbance and the storage modulus values at any given time were normalized with the hydrogen-bonded C═O peak absorbance and the storage modulus of the fully aged solution cast sample, respectively.

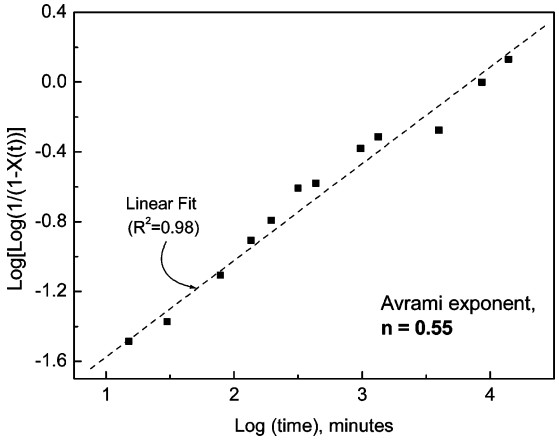

Figure 7. Linearized Avrami equation fit of the normalized storage modulus values presented in Figure 6.

rapidly over a period of 4 h, and a plateau value on the order of 10^8 Pa was achieved in about 20 h. Thus, the time required for the development of the microphase morphology in the bulk as well as on the free surface, where the AFM images were taken, is comparable. The normalized ATR−FTIR absorbance at 1700 cm^{-1} (from Figure 5) is also plotted in Figure 6 along with the normalized E' values. Upon comparison of these two data sets, it is clearly evident that the microphase morphology and the hard phase hydrogen-bonded network develop concurrently, indicating that these two different parameters are closely coupled.

Earlier, Wilkes and co-workers demonstrated that a loss of the microphase-separated morphology of selected commercial polyester- or polyether-based chain extended polyurethanes could be achieved by raising the temperature above the microphase separation transition temperature.[9−11] These investigators demonstrated by using a variety of techniques, such as DMA, DSC, and small-angle X-ray scattering, that upon lowering the temperature the morphology *recovered* with time. For the particular segmented polyurethanes investigated, major changes in the morphology took place within 3−5 h at ambient temperature. Smaller changes continued for ~2 weeks, beyond which no further changes were noted. Following those reports, other research groups have also observed similar time-dependent morphological behavior in related chain extended segmented polyurethanes.[12,13]

In the present study, the development of the long-range connectivity of the hard segments as observed by AFM and the concomitant rise in the E' of PTMO-*p*PDI-U described above demonstrate that the hard domains, which are crystalline, serve as reinforcing sites for the soft matrix. Further, it is hypothesized that the development of hard segment crystallinity (isothermal crystallization kinetics) should be closely coupled with the increase in the copolymer's ambient temperature storage modulus, E'. Such a first-order approximation seems reasonable in view of the low hard segment content of the sample and the ability of the hard segments to rapidly develop long-range connectivity. If the above hypothesis is true, then the E'−time response of PTMO-*p*PDI-U (Figure 6) might be described by the Avrami equation, which is often utilized to analyze isothermal crystallization kinetics behavior.[14] The Avrami equation is given by

$$1 - X_c(t) = \exp(-kt^n) \tag{1}$$

where $X_c(t)$ is the normalized volume fraction of the crystalline phase at t, the crystallization time, k is the preexponential constant, and n is referred to as the Avrami exponent. On the basis of the above discussion, the variable $X_c(t)$ is represented as

$$X_c = \frac{X_c(t)}{X_c(\infty)} \cong \frac{E'(t)}{E'(\infty)} \tag{2}$$

where $X_c(\infty)$ and $E'(\infty)$ are the normalized volume fraction of the crystalline phase and the storage modulus of the fully aged sample, respectively. Linearization of eq 1 yields

$$\log[-\log(1 - X_c)] = \log(k) + n \log(t) \tag{3}$$

From the linearized Avrami plot (Figure 7) it is evident that, indeed, the development of hard phase crystallinity is closely correlated to the rise in the copolymer's ambient temperature storage modulus. It is also interesting to note that the Avrami exponent, n, is equal to 0.55. In di- or triblock copolymers with crystallizable block(s), investigators have also noted Avrami exponent values of about 0.5 that resulted from experiments where the crystallization kinetics of the crystallizable block was monitored by DSC.[15−17] While several research groups[15−22] have observed this phenomenon in di- and triblock copolymers with the crystallizable block being the dispersed phase, the above results may perhaps constitute the first such observation in a segmented copolymer.

Conclusions

A segmented polyurethane with monodisperse hard segments based on the symmetric 1,4-phenylene diisocyanate was able to develop a microphase-separated morphology. Its hard phase, amounting to 14 wt %, was hydrogen bonded, crystalline, and extensively percolated. Thus, the material exhibited a high plateau storage modulus, which is an important requirement for elastomers intended for structural applications. Moreover, the ambient temperature modulus of the copolymer could be reasonably predicted by each of the selected three models developed for polymer composites reinforced by randomly dispersed fibers. In this material, the development of the morphology and the hard phase hydrogen-bonded network from a disordered state was a time-dependent phenomenon. The concurrent rise in the storage modulus of the copolymer could be

described by the Avrami equation, yielding an Avrami exponent of 0.55.

Acknowledgment. This material is based upon work supported in part by the U.S. Army Research Laboratory and the U.S. Army Research Office under Grant DAAD19-02-1-0275 Macromolecular Architecture for Performance (MAP) Multi-University Research Initiative.

References and Notes

(1) Hepburn, C. *Polyurethane Elastomers*; Elsevier Applied Science: New York, 1992.
(2) Legge, N. R., Holden, G., Schroeder, H. E., Eds.; *Thermoplastic Elastomers: A Comprehensive Review*, 1st ed.; Hanser Publishers: New York, 1987.
(3) Sheth, J. P.; Klinedinst, D. B.; Wilkes, G. L.; Yilgor, I.; Yilgor, E. *Polymer* **2005**, *46*, 7317−7322.
(4) Klinedinst, D. B.; Sheth, J. P.; Yilgor, E.; Yilgor, I.; Beyer, F. L.; Wilkes, G. L. American Chemical Society−Rubber Division, 167th Technical Meeting, 2005.
(5) Manuscript in preparation.
(6) Barikani, M.; Hepburn, C. *Cell. Polym.* **1987**, *6*, 41−45.
(7) Pan, N. *Sci. Eng. Compos. Mater.* **1996**, *5*, 63−72.
(8) Fetters, L. J.; Lohse, D. J.; Graessley, W. W. *J. Polym. Sci., Polym. Phys.* **1999**, *37*, 1023.
(9) Wilkes, G. L.; Bagrodia, S.; Humphries, W.; Wildnauer, R. *J. Polym. Sci., Polym. Lett. Ed.* **1975**, *13*, 321.
(10) Wilkes, G. L.; Wildnauer, R. *J. Appl. Phys.* **1975**, *46*, 4148.
(11) Wilkes, G. L.; Emerson, J. A. *J. Appl. Phys.* **1975**, *47*, 4261.
(12) Lagasse, R. R. *J. Appl. Polym. Sci.* **1977**, *21*, 2489.
(13) Hesketh, T, R.; Van Bogart, J. W. C.; Cooper, S. L. *Polym. Eng. Sci.* **1980**, *20*, 190.
(14) Mark, J. E., Ed.; *Physical Properties of Polymers Handbook*; American Institute of Physics: New York, 1996.
(15) Lotz, B., Kovacs, A. J. *Polym. Prepr.* **1969**, *10*, 820−825.
(16) Xu, J. T.; Ryan, A. J.; Mai, S. M.; Yuan, J. J.; Cheng, Y. Y. *J. Macromol. Sci., Part B: Phys.* **2004**, *43*, 685−695.
(17) Balsamo, V.; Urdaneta, N.; Perez, L.; Carrizales, P.; Abetz, V.; Muller, A. J. E. *Polym J.* **2004**, *40*, 1033−1049.
(18) Robitaille, C.; Prudhomme, J. *Macromolecules* **1983**, *16*, 665−671.
(19) Loo, Y. L.; Register, R. A. *Phys. Rev. Lett.* **2000**, *84*, 4120−4123.
(20) Zhu, L.; Mimnaugh, B. R.; Ge, Q.; Quirk, R. P.; Cheng, S. Z. D.; Thomas, E. L.; Lotz, B.; Hsiao, B. S.; Yeh, F.; Liu, L. *Polymer* **2001**, *42*, 9121−9131.
(21) Loo, Y. L.; Register, R. A.; Ryan, A. J.; Dee, G. T. *Macromolecules* **2001**, *34*, 8968−8977.
(22) Loo, Y. L.; Register, R. A.; Ryan, A. J. *Macromolecules* **2002**, *35*, 2365−2374.

MA051063A